

Proceeding Paper

Method for Determining Fracture Energy of a Polypropylene Coarse Lightweight Aggregate Concrete Beam Using Digital Image Correlation [†]

Sittati Musalamah ^{*}, Heru Purnomo and Nuraziz Handika 

Department of Civil Engineering, Faculty of Engineering, Universitas Indonesia, Depok 16424, Indonesia; heru.purnomo@ui.ac.id (H.P.); n.handika@ui.ac.id (N.H.)

^{*} Correspondence: smusalamah@unj.ac.id

[†] Presented at the 7th Mechanical Engineering, Science and Technology International Conference, Surakarta, Indonesia, 21–22 December 2023.

Abstract: This study aimed to propose a method for determining the fracture behavior of sand-coated polypropylene coarse aggregate lightweight concrete (PP-LWAC). To understand the fracture response, an experimental investigation is carried out on 36 beam specimens and PP-LWAC is prepared using sand-coated PP aggregate based on previous study. The mix proportion is designed to match with three different specified compressive strengths. The Work of Fracture Method (WFM) and Size Effect Method (SEM) is used to define the fracture parameters, proposing the relationship between the fracture parameters and the compressive strength. Additionally, the crack mechanism is studied using the Digital Image Correlation (DIC) method.

Keywords: lightweight aggregate; fracture parameters Work of Fracture Method Size Effect Method; Digital Image Correlation



Citation: Musalamah, S.; Purnomo, H.; Handika, N. Method for Determining Fracture Energy of a Polypropylene Coarse Lightweight Aggregate Concrete Beam Using Digital Image Correlation. *Eng. Proc.* **2024**, *63*, 19. <https://doi.org/10.3390/engproc2024063019>

Academic Editors: Waluyo Adi Siswanto, Sarjito, Supriyono, Agus Dwi Anggono, Tri Widodo Besar Riyadi and Taurista Perdana Syawitri

Published: 5 March 2024



Copyright: © 2024 by the authors. Licensee MDPI, Basel, Switzerland. This article is an open access article distributed under the terms and conditions of the Creative Commons Attribution (CC BY) license (<https://creativecommons.org/licenses/by/4.0/>).

1. Introduction

Polypropylene Coarse Lightweight Aggregate Concrete (PP-LWAC) is an innovative class of lightweight concrete, using polypropylene as a coarse aggregate. This material shows the shift towards more sustainable and environmentally friendly construction practices, according to several Sustainable Development Goals (SDGs), particularly those related to sustainable cities and communities, responsible consumption and production, as well as climate action. The use of polypropylene, often sourced from recycled plastics, reduces the waste stream and the overall weight of the concrete, leading to lower transportation emissions and minimal structural load.

Previous study has shown that the use of lightweight concrete offers advantages such as reduced structural component size, enhanced design flexibility, reduced dead load of structures, improved structural response to dynamic or seismic loads, and reduction in steel bars [1]. Additionally, it provides increased thermal insulation [2]. The application of lightweight concrete in structural elements also has positive effects, including improved ductility [3], increased cracking load [4], enhanced collapse load capacity, larger deflection values, and minimized crack width [5]. However, this material has a higher friction compared to normal concrete, as indicated by lower fracture energy value [6], limiting its use in the construction industry.

Although the use of polypropylene aggregate in concrete offers numerous advantages, careful consideration is required regarding its influence on structural integrity. One main aspect of assessing the durability and safety of this material is understanding the fracture mechanism. Generally, cracks are inherent properties of quasi-brittle materials such as concrete, which can rapidly lead to failure. Therefore, there is a need to investigate the fracture energy to fully understand the implications of using polypropylene aggregate.

This understanding is essential for predicting and mitigating potential failures in structures using PP-LWAC.

The methods that have been established for determining the fracture energy in concrete [7] are categorized into two primary methods; namely the Work of Fracture Method (WFM) and the Size Effect Method (SEM). WFM has been used for determining the fracture energy of various lightweight concrete types, including foam concrete [8], polypropylene fiber concrete [9], and limestone [10]. Meanwhile, SEM is widely applied for lightweight concrete using expanded clay aggregates [11]. Several studies have integrated both methods to ascertain the fracture energy of lightweight concrete, by combining WFM and SEM [6,12–14], as well as SEM and the Boundary Effect Method [15]. However, there is limited information on the fracture energy determination in sand-coated PP-LWAC.

Digital Image Correlation (DIC) is a non-invasive optical method that enables the monitoring of structures without inflicting damage. This method is effective in detecting and tracking crack initiation as well as progression to analyze fracture mechanisms [16–19]. Several studies have applied DIC to determine the fracture energy in various materials, including asphalt concrete [20], full-graded dam concrete specimens [21], and hydraulic concrete [22]. However, its application in investigating the fracture energy in lightweight concrete aggregates, particularly those composed of sand-coated polypropylene, has not been documented.

Based on the background above, this study aimed to investigate the fracture mechanism of sand-coated PP-LWAC using DIC. Initially, existing literature on the fracture energy determination method is reviewed, with a focus on WFM and SEM, as well as the application in various concrete types. This was followed by a detailing of the method used, emphasizing the innovative use of DIC as a non-invasive technique for observing crack propagation in lightweight concrete.

2. Proposed Method

Proposed method used for investigating the fracture energy in sand-coated PP-LWAC included WFM and SEM. Additionally, DIC was used to capture detailed visualizations of the crack initiation and propagation, as well as to analyze the fracture mechanisms.

2.1. Work of Fracture Method (WFM)

WFM is commonly used for determining the fracture energy in line with RILEM FMC-50 [23] and based on the Hillerborg cohesive crack model [24]. The determination of the fracture energy was carried out by a three-point bending test on a notched beam and calculated using the following Equation (1):

$$G_F = \frac{W_F}{(d - a_0)b} \quad (1)$$

where G_F is the total fracture energy in N/mm, while W_F denotes the total consumed fracture energy correlated with the area under the load–displacement curve, measured in N.mm. Additionally, b , d , and a_0 correspond to the width, height, and notch depth of the beam, respectively, each measured in mm.

The brittleness and ductility of concrete will be evaluated through the material characteristic length (L_{ch}) using Equation (2):

$$L_{ch} = \left(\frac{EG_F}{f_t^2} \right) \quad (2)$$

where L_{ch} , E , and f_t denote the characteristic length (mm), modulus of elasticity (GPa), and tensile strength (MPa), respectively. A higher L_{ch} value indicates that the concrete shows greater ductility, implying an enhanced ability to resist crack propagation.

2.2. Size Effect Method (SEM)

According to RILEM FMT-89 [25], SEM is recommended as an easier and simpler method for determining fracture energy. This method includes performing a three-point bending test on the geometrically similar notched beam of various sizes. In this method, the primary fracture parameters obtained are fracture energy (G_f), length of fracture-prone zone (C_f), brittleness number (β), fracture toughness (K_{IC}), and effective crack-tip opening displacement at maximum load (δ_C).

A five-step calculation process is carried out to accurately determine the fracture energy. The first step is to determine the weight compensation by calculating the peak load correction of P_0 using Equation (3):

$$P_j^0 = P_j + \frac{2S_j - L_j}{2S_j} m_j g_j = 1, \dots, n \quad (3)$$

where S and L are the distance between support and length of the specimen, respectively; m is the mass of the specimen; and g represents gravitational acceleration. The second step uses a linear regression analysis, which is conducted by plotting the ordinate Y and the abscissa X with:

$$X_j = d_j, Y_j = \left(\frac{bd_j}{P_j^0} \right)^2 \quad (4)$$

$$Y = AX + C \quad (5)$$

In which $X = d, Y = \left(\frac{1}{\sigma_N} \right)^2, d_0 = \frac{C}{A}, B = \frac{1}{\sqrt{C}}$.

The third step entails the determination of the specific fracture energy and effective length of fracture process zone:

$$G_f = \frac{g(\alpha_0)}{AE} \quad (6)$$

$$C_f = \frac{g(\alpha_0)}{g'(\alpha_0)} \times \frac{C}{A} \quad (7)$$

where G_f is the fracture energy in N/m , C_f is the effective length of the process zone in mm , E is Young's modulus of concrete, A is the slope of the line obtained from regression, C is the intersecting point of the y -axis with the regression line, $g(\alpha_0)$ is the dimensionless energy rate, which is function of structural geometry, and $g'(\alpha_0)$ is the first derivative with respect to the initial crack relative length ($\alpha_0 = \frac{a_0}{d}$). Akbari et al. [6] stated that $g(\alpha_0)$ and $g'(\alpha_0)$ are the functions that depend on the specimen geometry and are obtained as per LEFM.

The fourth step includes the calculation of mode I fracture toughness and effective crack-tip opening displacement:

$$K_{IC} = \sqrt{EG_f} \quad (8)$$

$$\delta_C = \frac{8K_{IC}}{E} \times \sqrt{\frac{C_f}{2\pi}} \quad (9)$$

where K_{IC} is in $MPa \cdot mm^{0.5}$ and δ_C in mm .

Nominal strength of geometrically similar specimens in SEM uses size effect law and can be calculated with:

$$\sigma_N = \frac{B}{\sqrt{1 + \beta}}, \beta = \frac{d}{d_0} \quad (10)$$

where σ_N is the nominal strength in MPa and parameter β is the Bazant and Kazemi's brittleness number [26]. When β is greater than 10, linear elastic fracture mechanics (LEFM) is used to indicate the failure. When the value is less than 0.1, the failure determination can use plastic limit analysis. Among these limit values, the determination of the failure is

expressed as fracture mechanics. For specimens with a similar geometry in two dimensions, σ_N can be calculated using Equation (11):

$$\sigma_N = C_n \frac{P_u}{bd} \quad (11)$$

where P_u is the maximum load (N), C_u is the constant coefficient, b is the beam width (mm), and d is the beam depth (mm).

2.3. Digital Image Correlation (DIC)

DIC commences with capturing a reference image of a sample before loading. Throughout the loading or testing phase, continuous images of the specimen are captured. Subsequently, software that functions as an image correlation is used during the testing process for comparison with reference image. The comparison results show the deformation or movement the specimen passes through during the test [20]. A stochastic contrast speckle pattern, which must first be applied to the surface under study, is used to measure deformations in line with the DIC method. This pattern is crucial for accurate measurement of deformations, requiring adherence to certain criteria to ensure high-confidence experimental results and minimal noise. The criteria include high contrast, constant speckle sizes, surface filling, isotropy, as well as randomness [27]. Moreover, adherence to these standards ensures that the DIC method provides reliable and detailed insights into the material's behavior under stress, serving as an invaluable tool in the study of fracture mechanics in sand-coated PP-LWAC.

3. Experimental Program

3.1. Materials

In this study, the fine aggregate used is sourced from Cimangkok, West Java, Indonesia. Furthermore, the fine aggregate has a bulk specific gravity of 2.54 and a fineness modulus of 2.686, with a particle size less than 9.5 mm. The superplasticizer (SP) will be incorporated as the mixture material for all water/cement (w/c) ratios to enhance fresh concrete workability. This additive has a specific gravity ranging between 1.18 and 1.2 at 27 °C.

The Portland Cement Composite is used as the primary binder and polypropylene (PP) plastic waste will be processed into coarse aggregate. The initial form of this uncoated plastic aggregate, resembling the design created by G. Pamudji et al. [28] is shown in Figure 1a. Typically, the largest pieces of the aggregate measures 10 mm in thickness, 20 mm in length, and 20 mm in width. The production process for the coated aggregate follows a similar procedure, where the plastic aggregate is melted and molded under hydraulic pressure using an automatic temperature control manual injection plastic machine, at a melting point range of 130°C ± 10°C. After formation, the plastic aggregate is cooled, and the uncoated sample is covered with hot sand to produce the final sand-coated plastic aggregate, as shown in Figure 1b.



Figure 1. Polypropylene coarse aggregate: (a) uncoated plastic aggregate and (b) plastic aggregate coated with sand.

3.2. Mix Design and Test Specimen Preparation

An experimental program will be designed in this study, following the procedures stated in previous study [29]. The design consisted of three concrete mixes corresponding to the target strength class, as shown in Table 1. The dry mix concrete will be used as the normal concrete, serving as the control specimen, which provided a baseline for comparison with the modified concrete mixes. The production process of the concrete refers to ASTM C192.

Table 1. Mix composition of the PP coarse aggregate concrete.

Target Strength Class	w/c Ratio	Cement	Sand	PP Aggregate	Water	SP
17–18.9 MPa	0.29	1	2	2.6	0.85	0.60%
19–20.9 MPa	0.28	1	2	2	0.81	0.70%
>21 MPa	0.286	1	2	1.8	0.9	0.80%

3.3. Test Procedure

In this study, nine cylindrical specimens measuring 150 × 300 mm will be fabricated for each concrete mix series. Several tests are conducted consisting of three specimens each allocated for measuring modulus of elasticity (E), determining Poisson’s ratio, and tensile strength test (f_t) in accordance with ASTM C469. Additionally, three smaller cylindrical specimens measuring 100 × 200 mm will be prepared for each mix to determine the compressive strength (f_c) base” on ‘STM C39.

To evaluate the fracture parameters using WFM, three notched beams will be crafted for every target strength class. The beams have dimensions of 100 × 100 × 840 mm (depth × width × length) and an 800 mm span. An illustrative example of concrete beams prepared for WFM testing is shown in Figure 2a. On the bottom fiber (material under tension), a steel plate will be positioned centrally on the beam to introduce a vertical notch, with a uniform width of 5 mm. The ratio of the vertical notch depth to the three beam’s depth is set at 0.5 ($a_0 = 0.5d$), as depicted in the beam framework shown in Figure 2b. During testing, a displacement-controlled load is employed, applying a concentrated load at the center of the beam’s span. Throughout each test, the load applied to the beam and deformations of specimens were simultaneous, ensuring a comprehensive understanding of the material’s fracture behavior under stress.

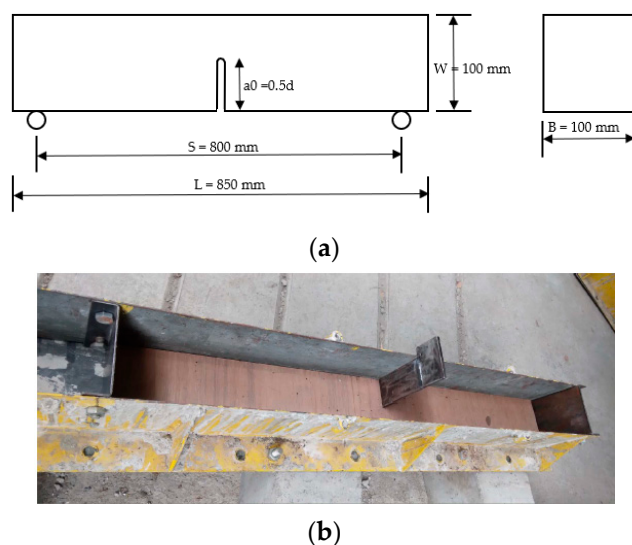


Figure 2. Notched beam specimens: (a) specimens for WFM analyzing and (b) framework of notched beam.

A set of notched beams, designed according to RILEM FMT-89 [25], will be further fabricated to assess the fracture parameters using SEM. Table 2 shows the specific dimen-

sions of the beams scaled in a ratio of 0.75:1:1.25, with three beams will be fabricated for each target strength category. Subsequently, a continuous vertical notch with a depth of $a_0 = 0.2d$ will be introduced at the midspan of each beam by embedding a steel plate into the bottom fiber during the concrete casting process. A universal testing machine (UTM) with a maximum capacity of 50 kN will be used to test all notched beams under three-point static loading. The beams will be loaded at a constant rate of 0.1 mm/min for SEM and 0.5 mm/min at WFM.

Table 2. Summary of experimental design.

Specimens	Standard	Number of Repetitions Per Mix	Achievable Parameter
150 × 300 mm ³ cylindrical specimen	ASTM C496	three three three	Modulus of elasticity Direct tensile strength Poisson's Ratio
100 × 200 mm ³ cylindrical specimen	ASTM C39	three	Compressive strength
100 × 100 × 840 mm ³ beam specimen	RILEM FMC-50 RILEM FMT-89	three three	Fracture toughness (WFM) Fracture toughness (SEM)
75 × 75 × 630 mm ³ beam specimen	RILEM FMT-89	three	Fracture toughness (SEM)
125 × 125 × 1050 mm ³ beam specimen	RILEM FMT-89	three	Fracture toughness (SEM)

The test procedure for DIC includes the use of a high-speed digital camera to capture a series of digital pictures of the concrete specimen. Using black ink, each speckle on the test specimen's surface is marked individually [21]. Subsequently, the camera is set up vertically two meters from the specimen's surface and mounted on a tripod, with LED cold light placed in front serving as the light source. Before testing, the DIC system is calibrated to ensure accurate deformation measurements. A reference image is captured to assess the speckle quality and confirm the accuracy of the calibration's precision. To ensure that sufficient photos are obtained for recording the evolution of the crack, image acquisition frequency is adjusted during the test based on the loading rate. This sequential method ensures a detailed and accurate recording of the fracture process, providing valuable insights into the material's behavior.

4. Analysis Mechanism

4.1. Mechanical Properties

A total of 45 cylindrical and 45 prism specimens will be fabricated in the Structural and Material Laboratory at the Universitas Indonesia. The fabrication process is carried out using two types of mixes, namely normal weight concrete (NWC) and lightweight concrete (LWC). The mechanical properties of the concrete, including modulus elasticity, Poisson's Ratio, and direct tensile strength, will be derived from the experiment. A comparative analysis between the NWC and LWC will be conducted to determine their performance. Subsequently, the analysis of the material properties is carried out by observing the general trends occurring in each of the mechanical characteristics and investigating influencing factors. The results showing the mechanical properties will be systematically presented through figures and tables, providing a clear and comprehensive understanding of how the two concrete types compare in terms of their characteristics.

Total fracture energy (G_F), or the energy required to propagate a crack with a unit surface area, is determined using WFM. This study will show variations in G_F for both NWC and LWC across different target strength classes, investigating all potential factors. The data obtained will be compared with other studies to contextualize the results within the broader study landscape. Subsequently, a relationship will be proposed between G_F and

the compressive strength of LWC, specifically sand-coated polypropylene coarse aggregate lightweight concrete (PP-LWAC).

The characteristic length L_{ch} is a key parameter in WFM for determining the ductility and brittleness of concrete. This parameter is intrinsically correlated to the length of the fracture process zone (FPZ) in the fictitious crack model. During the analysis, Equation (2) will be used to calculate L_{ch} , and the result will be shown in the figures for further analysis. Moreover, a nonlinear regression analysis will be conducted to express L_{ch} (mm) as a function of the compressive strength f'_c (MPa) of LWC.

4.2. Analysis of Fracture Parameters based on SEM

In accordance with the guidelines provided by RILEM FMT-89 [25], the peak load calculation for NWC and LWC specimens is expected to include adjustments for the weight of the beam. This correction is crucial to ensure that the peak load accurately reflects the specimens' capacity to withstand applied forces. During the analysis, Equation (3) will be used to modify the peak loads for the NWC and LWC specimens. Moreover, a linear regression analysis, in line with RILEM TC89-FMT guidelines, will be conducted to ascertain the primary fracture parameters in SEM, including the initial fracture energy (G_f), the effective length of the fracture process zone (C_f), and the fracture toughness (K_{IC}), among others. Subsequently, the relationship between the initial fracture energy G_f (N/mm) and compressive strength f'_c (MPa) for LWC is expressed by an equation. The results are compared with other studies to validate the conclusions.

4.3. DIC Analysis of Fracture Behavior

During the fracture test, strain and displacement measurements will be obtained from the captured image through DIC method. A two-dimensional (2D)-DIC setup will be used with a Fuji film X-A3 camera and two light sources. Using the reference image as a guide, the DIC analysis tracks the speckles in distorted images. Subsequently, GOM Correlate 2021 software, a renowned tool in the field of digital image processing, will be used to analyze the images captured.

By using the same software, the postprocessing will be performed to extract the DIC analysis result. The horizontal displacements of the notch can be extracted from the specimens' surface using a line-type inspection gauge. The line drawn at the crack mouth opening displacement (CMOD) clip gauge level on the processed image is divided into various index points, to extract all the readings. As the points in the middle part overlap with the notch opening, the values of displacement indicate zero. Subsequently, the experimental clip gauge and the load-CMOD curves from DIC will be compared and presented in a figure.

5. Conclusions

In conclusion, this study design an extensive experimental program to investigate the fracture behavior of NWC and LWC using a combination of WFM and SEM, as stated by RILEM FMT-89. Adjustments for the weight of beam specimens and a series of linear regression analyses will be conducted to determine the primary fracture parameters and establish a relationship between fracture energy and compressive strength for LWC. The DIC method, using a 2D setup with a Fuji film X-A3 camera, will be used to capture strain and displacement measurements, which will be analyzed by software. Comparative analysis between experimental clip gauge data and DIC-derived load-CMOD curves will be used to validate the efficacy of the DIC method. This comprehensive method will focus on providing a better understanding of fracture mechanics in concrete, contributing valuable insights for the development of more resilient and sustainable construction materials.

Author Contributions: Conceptualization and methodology, H.P.; software development, H.P. and N.H.; validation, H.P. and N.H.; formal analysis, S.M. and N.H.; investigations, S.M. and N.H.; resources, S.M., H.P., N.H.; data curation S.M.; writing-original draft preparation, S.M.; writing-review and editing, N.H.; visualization; S.M. and N.H.; supervision and funding acquisition, H.P. and N.H. All authors have read and agreed to the published version of the manuscript.

Funding: This study received no external funding.

Institutional Review Board Statement: Not applicable.

Informed Consent Statement: Not applicable.

Data Availability Statement: The data presented in this study are available on request from the corresponding author.

Conflicts of Interest: The authors declare no conflicts of interest.

References

1. Kulbhushan, K.; Kumar, S.; Chaudhary, R.; Ahmad, S.; Gupta, S.; Chaurasia, R. A Contextual Analysis of the advantages by using lightweight concrete blocks as substitution of bricks. *Int. Res. J. Eng. Technol.* **2018**, *5*, 6.
2. Poonyakan, A.; Rachakornkij, M.; Wecharatana, M.; Smittakorn, W. Potential use of plastic wastes for low thermal conductivity concrete. *Materials* **2018**, *11*, 1938. [[CrossRef](#)] [[PubMed](#)]
3. Adnan, H.M.; Dawood, A.O. Strength behavior of reinforced concrete beam using re-cycle of PET wastes as synthetic fibers. *Case Stud. Constr. Mater.* **2020**, *13*, e00367. [[CrossRef](#)]
4. Mohammed, A.A.; Rahim, A.A.F. Experimental behavior and analysis of high strength concrete beams reinforced with PET waste fiber. *Constr. Build. Mater.* **2020**, *244*, 118350. [[CrossRef](#)]
5. Noori, A.Q.N.; Numan, H.A. Behavior of sustainable reinforced concrete building containing waste plastic and fibers. In *IOP Conference Series: Materials Science and Engineering*; IOP Publishing: Bristol, UK, 2020; Volume 870, p. 012094.
6. Akbari, M.; Tahamtan, M.H.N.; Fallah-Valukolaee, S.; Herozi, M.R.Z.; Shirvani, M.A. Investigating fracture characteristics and ductility of lightweight concrete containing crumb rubber by means of WFM and SEM methods. *Theor. Appl. Fract. Mech.* **2022**, *117*, 103148. [[CrossRef](#)]
7. Khalilpour, S.; BaniAsad, E.; Dehestani, M. A review on concrete fracture energy and effective parameters. *Cem. Concr. Res.* **2019**, *120*, 294–321. [[CrossRef](#)]
8. Falliano, D.; De Domenico, D.; Sciarrone, A.; Ricciardi, G.; Restuccia, L.; Ferro, G.; Tulliani, J.-M.; Gugliandolo, E. Influence of biochar additions on the fracture behavior of foamed concrete. *Frat. Integrità Strutt.* **2020**, *14*, 189–198. [[CrossRef](#)]
9. Li, J.; Wan, C.; Zhang, X.; Niu, J. Fracture property of polypropylene fibre-reinforced lightweight concrete at high temperatures. *Mag. Concr. Res.* **2020**, *72*, 1147–1154. [[CrossRef](#)]
10. Yang, J.; Song, C.; Wang, Q. Comparative analysis of the effects of aggregates and fibres on the fracture performance of lightweight aggregate concrete based on types I and II fracture test methods. *Theor. Appl. Fract. Mech.* **2022**, *117*, 103202. [[CrossRef](#)]
11. Afzali-Naniz, O.; Mazloom, M.; Karamloo, M. Effect of nano and micro SiO₂ on brittleness and fracture parameters of self-compacting lightweight concrete. *Constr. Build. Mater.* **2021**, *299*, 124354. [[CrossRef](#)]
12. Mehrab, A.H.; Esfahani, M.R. Experimental Study on Size Effect and Fracture Properties of Polypropylene Fiber Reinforced Lightweight Aggregate Concrete. *Period. Polytech. Civ. Eng.* **2022**, *66*, 1278–1293.
13. Dabbaghi, F.; Fallahnejad, H.; Nasrollahpour, S.; Dehestani, M.; Yousefpour, H. Evaluation of fracture energy, toughness, brittleness, and fracture process zone properties for lightweight concrete exposed to high temperatures. *Theor. Appl. Fract. Mech.* **2021**, *116*, 103088. [[CrossRef](#)]
14. Karamloo, M.; Afzali-Naniz, O.; Doostmohamadi, A. Impact of using different amounts of polyolefin macro fibers on fracture behavior, size effect, and mechanical properties of self-compacting lightweight concrete. *Constr. Build. Mater.* **2020**, *250*, 118856. [[CrossRef](#)]
15. Nikbin, I.M.; Farshamizadeh, M.; Jafarzadeh, G.A.; Shamsi, S. Fracture parameters assessment of lightweight concrete containing waste polyethylene terephthalate by means of SEM and BEM methods. *Theor. Appl. Fract. Mech.* **2020**, *107*, 102518. [[CrossRef](#)]
16. Parmadi, B.J.; Handika, N.; Sutanto, D.; Sentosa, B.O. Recycled aggregate concrete beam: Experimental study using digital image correlation (DIC) and numerical study using multi-fibre Timoshenko beam element in CAST3M. In *AIP Conference Proceedings*; AIP Publishing: Damansara, Malaysia, 2023; Volume 2847.
17. Ernawan, E.; Sjah, J.; Handika, N.; Astutiningsih, S.; Vincens, E. Mechanical Properties of Concrete Containing Ferronickel Slag as Fine Aggregate Substitute Using Digital Image Correlation Analysis. *Buildings* **2023**, *13*, 1463. [[CrossRef](#)]
18. Deltanto, A.D.; Handika, N.; Sentosa, B.O.B. Response of load-displacement on cubical sample of Oil-Palm shell with fly ash concrete using digital image correlation system. In *AIP Conference Proceedings*; AIP Publishing: Depok, Indonesia, 2021; Volume 2376.
19. Hongsan, K.; Melhan, M.; Handika, N.; Sentosa, B.O.B. Parameterization of Oil Palm Shell Concrete on Numerical Damage Model Based on Laboratory Experiment using Digital Image Correlation. *J. Phys. Conf. Ser.* **2021**, *1858*, 012029. [[CrossRef](#)]

20. Sudarsanan, N.; Zeng, Z.A.; Kim, Y.R. Laboratory investigation into the crack propagation mechanism of geosynthetic reinforced asphalt concrete using digital image correlation technique. *Int. J. Pavement Eng.* **2023**, *24*, 2251079. [[CrossRef](#)]
21. Bu, J.; Wu, X.; Xu, H.; Chen, X. The rate effect on fracture mechanics of dam concrete based on DIC and AE techniques. *J. Strain Anal. Eng. Des.* **2022**, *57*, 496–510. [[CrossRef](#)]
22. Ning, Y.; Ye, L.; Bai, L.; Xie, C.; Xu, H. Experimental Study on Fracture Properties of Hydraulic Concrete with Different Crack-Depth Ratios Based on Acoustic Emission and DIC Techniques. *Adv. Mater. Sci. Eng.* **2022**, *2022*, 8771674. [[CrossRef](#)]
23. Recommendation, R.D. Determination of the fracture energy of mortar and concrete by means of three-point bend tests on notched beams. *Mater. Struct.* **1985**, *18*, 285–290.
24. Hillerborg, A.; Modéer, M.; Petersson, P.-E. Analysis of crack formation and crack growth in concrete by means of fracture mechanics and finite elements. *Cem. Concr. Res.* **1976**, *6*, 773–781. [[CrossRef](#)]
25. D’Essai, M.; Mé, T.; De La Rilem, P. Size-effect method for determining fracture energy and process zone size of concrete. *Mater. Struct.* **1990**, *1*, 7.
26. Bazant, Y.; Kazemi, M. Determination of fracture energy, process zone length and brittleness number from size effect, with application to rock and concrete. *Int. J. Fract.* **1990**, *44*, 111–131. [[CrossRef](#)]
27. Blikharsky, Y.; Koptiika, N.; Khmil, R.; Blikharsky, Z. Digital Image Correlation Pattern for Concrete Characteristics—Optimal Speckle. In *International Conference Current Issues of Civil and Environmental Engineering Lviv-Košice-Rzeszów*; Springer: Berlin/Heidelberg, Germany, 2013; pp. 22–31.
28. Pamudji, G.; Purnomo, H.; Katili, I.; Imran, I. The use of plastics waste as coarse aggregates for moderate strength concrete. In *Proceedings of the 6th Civil Engineering Conference in Asia Region: Embracing the Future through Sustainability*, Hotel Borobudur, Jakarta, 20–22 August 2013; pp. 602–978.
29. Perdani. *Kajian Numerik Pull-Out Beton Ringan Beragregat Polipropilen Menggunakan Variasi Diameter Tulangan Dengan Fokus Eksperimen Pada Tes Tekan Silinder*. Undergraduate Thesis, Universitas Indonesia, Depok, Indonesia, 2017.

Disclaimer/Publisher’s Note: The statements, opinions and data contained in all publications are solely those of the individual author(s) and contributor(s) and not of MDPI and/or the editor(s). MDPI and/or the editor(s) disclaim responsibility for any injury to people or property resulting from any ideas, methods, instructions or products referred to in the content.